

## PRE- AND POST-SYNAPTIC MECHANISMS OF SYNAPTIC STRENGTH HOMEOSTASIS REVEALED BY SLOWPOKE AND SHAKER K<sup>+</sup> CHANNEL MUTATIONS IN *DROSOPHILA*

J. LEE,<sup>a</sup> A. UEDA<sup>b</sup> AND C.-F. WU<sup>a,b\*</sup>

<sup>a</sup>Interdisciplinary Program in Neuroscience, University of Iowa, Iowa City, IA 52242, USA

<sup>b</sup>Department of Biology, University of Iowa, Iowa City, IA 52242, USA

**Abstract**—We report naturally occurring, systematic variations in synaptic strength at neuromuscular junctions along the dorsal–ventral (D–V) axis of the *Drosophila* larval body wall. These gradual changes were correlated with differences in presynaptic neurotransmitter release regulated by nerve terminal excitability and in postsynaptic receptor composition influencing miniature excitatory junctional potential (mEJP) amplitude. Surprisingly, synaptic strength and D–V differentials at physiological Ca<sup>2+</sup> levels were not significantly altered in *slowpoke* (*slo*) and *Shaker* (*Sh*) mutants, despite their defects in two major repolarizing forces, Ca<sup>2+</sup>-activated Slo (BK) and voltage-activated Sh currents, respectively. However, lowering [Ca<sup>2+</sup>]<sub>o</sub> levels revealed greatly altered synaptic mechanisms in these mutants, indicated by drastically enhanced excitatory junctional potentials (EJPs) in *Sh* but paradoxically reduced EJPs in *slo*. Removal of Sh current in *slo* mutants by 4-aminopyridine blockade or by combining *slo* with *Sh* mutations led to strikingly increased synaptic transmission, suggesting upregulation of presynaptic Sh current to limit excessive neurotransmitter release in the absence of Slo current. In addition, *slo* mutants displayed altered immunoreactivity intensity ratio between DGluRIIA and DGluRIIB receptor subunits. This modified receptor composition caused smaller mEJP amplitudes, further preventing excessive transmission in the absence of Slo current. Such compensatory regulations were prevented by *rutabaga* (*rut*) adenylyl cyclase mutations in *rut slo* double mutants, demonstrating a novel role of *rut* in homeostatic plasticity, in addition to its well-established function in learning behavior. © 2008 IBRO. Published by Elsevier Ltd. All rights reserved.

**Key words:** synaptic strength, dorsal–ventral differentials, *rutabaga* adenylyl cyclase, cAMP, membrane excitability, postsynaptic receptor composition.

Natural variations in synaptic strength, or differential responses of postsynaptic targets to presynaptic inputs, play

\*Correspondence to: C.-F. Wu, Department of Biology, 231 Biology Building, University of Iowa, Iowa City, IA 52242, USA. Tel: +1-319-335-1091; fax: +1-319-335-1103.

E-mail address: [chun-fang-wu@uiowa.edu](mailto:chun-fang-wu@uiowa.edu) (C.-F. Wu).

**Abbreviations:** AC, adenylyl cyclase; A–P, anterior–posterior; *cac*, *cacophony*; ChTx, charybdotoxin; CREB, cAMP response element-binding protein; Dlg, Discs-Large; D–V, dorsal–ventral; EJP, excitatory junctional potential; FasII, Fasciclin II; I<sub>A</sub>, transient A-type K<sup>+</sup> current; IIA/IIB, DGluRIIA/DGluRIIB; mEJP, miniature excitatory junctional potential; NMJs, neuromuscular junctions; PKA, cAMP-dependent protein kinase; *rut*, *rutabaga*; *Sh*, *Shaker*; Sh, Shaker; *slo*, *slowpoke*; Slo, Slowpoke; WT, wild type; 4-AP, 4-aminopyridine.

0306-4522/08/\$32.00+0.00 © 2008 IBRO. Published by Elsevier Ltd. All rights reserved.

doi:10.1016/j.neuroscience.2008.04.043

crucial roles in matching the efficacy of individual synapses with different levels of activity demands. This mechanism is important for precise information transfer in neural circuits, in particular to support the functional organization of effectors in the various body plans. A well-studied example is the tonotopic processing of auditory information. There is a gradient of Ca<sup>2+</sup>-activated BK or Slowpoke (Slo) K<sup>+</sup> channel-mediated I<sub>KCa</sub> in sensory hair cells controlling tuning frequency along the base-to-apex axis of the cochlea (Fettiplace and Fuchs, 1999). In addition, differential expression of Shaker (Sh) voltage-activated K<sup>+</sup> (K<sub>v</sub>1) channels contributes to tonotopic processing of auditory information corresponding to a gradient of membrane excitability and synaptic transmission in the chicken nucleus magnocellularis (Fukui and Ohmori, 2004) and in the rat lateral superior olive (Barnes-Davies et al., 2004). These examples highlight the importance of K<sup>+</sup> channels in establishing natural gradients of neuronal activity and synaptic strength.

Another important aspect of regulation of synaptic strength is homeostatic maintenance of synaptic strength in individual neurons within a particular circuit. Neurons are able to restore proper synaptic functions when the neural circuits are destabilized following perturbations in membrane excitability, in neurotransmitter release machinery, in postsynaptic receptor functions, or in synaptic growth. For example, chronic blockade by TTX or enhancement by GABA receptor antagonists of mammalian neuronal activity in culture leads to a compensatory increase or decrease in postsynaptic response amplitude via regulation of AMPA receptor accumulation (O'Brien et al., 1998; Turrigiano et al., 1998). Similar homeostatic regulation occurs at *Drosophila* neuromuscular junctions (NMJs). A change in postsynaptic activity by expressing a persistent outward K<sup>+</sup> current, causing a hyperpolarized resting potential, results in a compensatory increase in presynaptic neurotransmitter release (Paradis et al., 2001). Mutations that decrease postsynaptic receptor density lead to an increase in presynaptic neurotransmitter release (Petersen et al., 1997). In addition, compensatory increases in synaptic areas and active zone numbers are induced by reduced number of synaptic varicosities to match the demand of target muscles (Stewart et al., 1996).

It has not been established how differential synaptic strength according to different body plans is related to homeostatic mechanisms following perturbations of synaptic strength. Here we document naturally occurring variations in synaptic strength along the dorsal–ventral

(D-V) body axis in the body wall of *Drosophila* larvae that correlate with differential expression of Sh  $K^+$  currents affecting presynaptic neurotransmitter release and with regulation of postsynaptic receptor composition. Mutational and pharmacological analyses reveal that, in the absence of major repolarizing Slo  $K^+$  channels, synaptic strength and its D-V differentials are still maintained homeostatically through presynaptic upregulation of Sh currents and postsynaptic alterations in receptor composition. Mutations in *rutabaga* (*rut*) adenylate cyclase (AC) prevent these homeostatic adjustments in *rut slo* double mutants, indicating that cAMP is central to the homeostatic plasticity in addition to its well-known roles in behavioral plasticity.

## EXPERIMENTAL PROCEDURES

### Fly stocks

The fly stocks used in this study include: wild type (WT) Canton-S (CS);  $K^+$  channel mutants, including *slowpoke* (*slo*) (*slo*<sup>1</sup>, *slo*<sup>98</sup>, and *slo*<sup>4</sup>), *Shaker* (*Sh*) (*Sh*<sup>M</sup> and *Sh*<sup>133</sup>), and *Sh*::*slo* (*Sh*<sup>133</sup>::*slo*<sup>1</sup> and *Sh*<sup>M</sup>::*slo*<sup>98</sup>), and AC mutants *rut* (*rut*<sup>1</sup> and *rut*<sup>1084</sup>) and *rut slo* (*rut*<sup>1</sup>::*slo*<sup>1</sup> and *rut*<sup>1</sup>::*slo*<sup>1/slo</sup><sup>4</sup>). Data collected from different alleles

of *slo* and *Sh* indicate similar physiological phenotypes (see Table S1 in the Supplement Data). Thus, results from the different alleles are combined in analysis to increase statistical power. All these stocks were raised in the presence of conventional fly medium and maintained at room temperature.

### Preparations and electrophysiology

Preparation of wandering third instar larvae and intracellular recordings of excitatory junctional potentials (EJPs) were performed as described previously (Ueda and Wu, 2006). Evoked EJPs upon segmental nerve stimulation were recorded from abdominal segments 3 through 6, mostly from 4th and 5th segments, in HL3.1 saline (Feng et al., 2004) containing 0.2 mM of  $Ca^{2+}$ , unless specified. For the analysis of D-V disparity, EJPs were sampled from multiple muscles in a single hemisegment (mostly from the 4th and 5th abdominal segments) per larva (Fig. 1B) to ensure stable muscle conditions throughout the experiment. The EJP amplitude from muscles 6/7 (V) was divided by that from muscles 1/9 (D) within the same hemisegment of body wall to calculate the EJP ratio (V/D). Miniature excitatory junctional potentials (mEJPs) with the resting membrane potential lower than  $-60$  mV were analyzed by MiniAnalysis software (Synaptosoft Inc., Fort Lee, NJ, USA). Quantal content was calculated either by dividing the mean EJP amplitude by the mean mEJP amplitude at 0.2 mM  $Ca^{2+}$ , or by calculating the log (1/failure rate) during 200 consecutive stim-

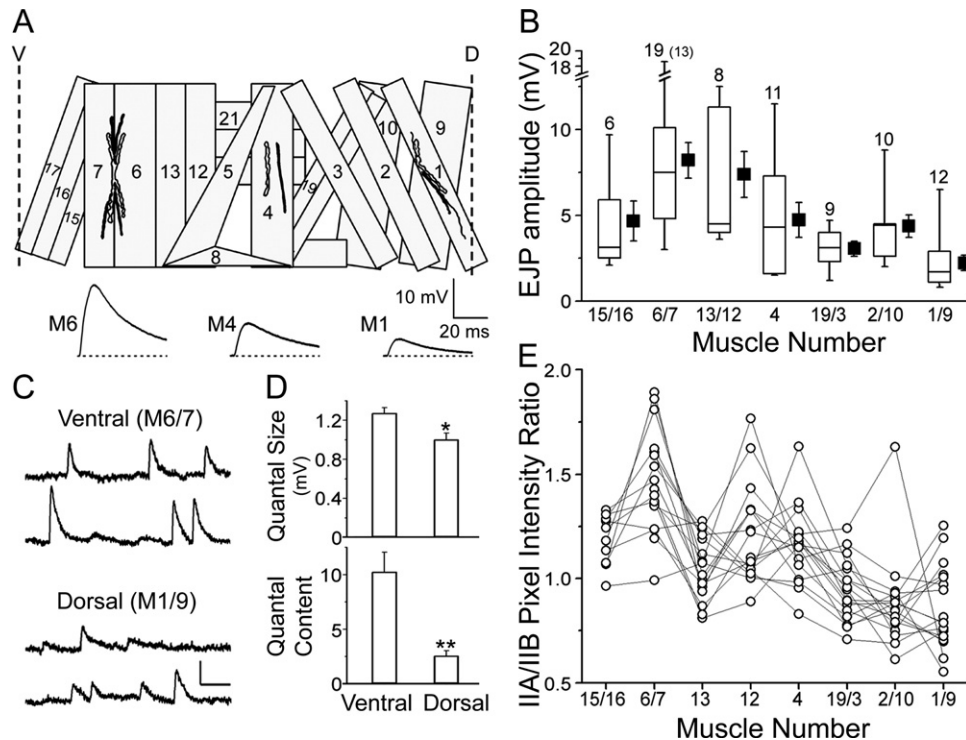


**Fig. 1.** Naturally occurring D-V disparity in EJP amplitudes correlated with differential regulation of presynaptic neurotransmitter release, postsynaptic receptor composition, and mEJP amplitudes. (A) Larval body-wall musculature within a single hemisegment from the ventral (V) to dorsal (D) midline of a third instar larva, with NMJs (isomorphic) on muscles 6, 4, and 1 and corresponding representative EJPs. The numbering system for the identified muscles is shown. (B) Pooled EJP amplitude data from muscles in the abdominal hemisegments are shown in the box plots together with mean  $\pm$  S.E.M. values with respect to their locations along the D-V axis. For each larva, five to eight muscles in a single hemisegment are sampled. The total number of muscle fibers is indicated (equivalent to the number of larvae except for muscles 6/7, 19 muscle fibers from 13 larvae). The box plot in this and following figures represents 25 through 75% with median and 5 and 95% indicated by bars. (C) Two representative traces of spontaneous mEJPs in WT are shown for ventral (M6/7) and dorsal (M1/9) NMJs. Scale bar = 1 mV and 100 ms. (D) Average quantal size (mEJP amplitude) (top) and quantal content (bottom) at ventral (M6/7) and dorsal (M1/9) NMJs in WT. Note a significantly smaller quantal size and quantal content at dorsal NMJs. \*  $P < 0.05$  and \*  $P < 0.01$ , *t*-test for ventral vs. dorsal NMJs. (E) Relative ratio of DGluRIIA/DGluRIIB (IIA/IIB) immunoreactivity visualized by double-labeling at the same type Ib NMJs reveals gradual changes along the D-V axis, resembling the D-V profile of EJP amplitude shown in (B) (see Experimental Procedures). Seventeen hemisegments in five larvae.

Download English Version:

<https://daneshyari.com/en/article/4340395>

Download Persian Version:

<https://daneshyari.com/article/4340395>

[Daneshyari.com](https://daneshyari.com)